

HYDRODYNAMIC ENTRANCE REGION FLOW OF A PARALLEL PLATE CHANNEL

by 4589

WEI-CHUNG CHEN

B. S. National Taiwan University, 1968

A MASTER'S REPORT

submitted in partial fulfillment of the

requirements for the degree

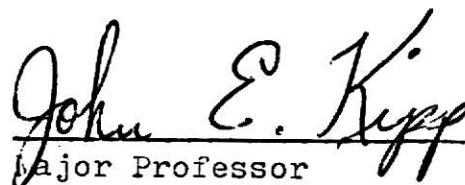
MASTER OF SCIENCE

Department of Applied Mechanics

KANSAS STATE UNIVERSITY
Manhattan, Kansas

1970

Approved by:


Major Professor

LD
2668
R4
1970
C4802
c.2

CONTENTS

	Page
I INTRODUCTION	1
II LITERATURE SURVEY	2
III ANALYSIS	5
IV RESULTS	11
V REFERENCES	17
APPENDICES	
A. Nomenclature	18
B. Flow Chart for Finding u^+ , v^+ , $\frac{dp^+}{dx^+}$	19
C. Program Listing with Selected Output	20

LIST OF FIGURES

	Page
Fig. 1. Geometry of duct-entrance region	5
Fig. 2. Pattern of points	7
Fig. 3. Velocity profiles	13
Fig. 4. Velocity profiles	14
Fig. 5. Pressure distribution	14

LIST OF TABLES

	Page
Table 1. Comparison of Results for u^+	15
Table 2. Comparison of Results for v^+	16

I INTRODUCTION

When a viscous fluid enters a conduit the velocity distribution and pressure gradient change. The flow in this inlet section is the so-called hydrodynamic entrance region flow.

Several approximate methods have been employed to investigate the entrance region flow problem. These being the matching method, the momentum integral method, the linearization method and the finite-difference method.

In this report a derivation of a finite-difference method for steady state, laminar flow between parallel plates is presented. The numerical solution obtained by a digital computer is also reported.

II LITERATURE SURVEY

A study of the development of the velocity profile has been investigated for the last hundred years. Although the governing differential equations for the entrance region flow may be easily written, their exact analytical solutions have not so far been found. However, various approximation methods of solution have been employed to solve the entrance region flow problem. The approximate methods may be classified into four categories - the momentum integral, linearization, matching, and finite-difference methods.

In the momentum integral method the flow is divided into a boundary layer part near the wall and a potential flow part in the central region. A parabolic velocity profile or any other similar velocity profile is assumed in the boundary layer and is joined with the central region velocity profile which is assumed to be a straight line. A momentum integral equation is derived based on the momentum conservation principle. This approach was devised and applied by Schiller[1] in 1922 for flow in a circular tube and is similar to the Karman-Pohlhausen momentum integral method applied to a flat plate.

In the linearization method the inertia terms of boundary layer equations are linearized. This class of solutions was originated and applied by Langhaar[2] in 1940 for steady flow in a straight tube. Although the solutions derived from this method are more accurate than that of Schiller's[1] method, the computational procedure is much more complicated than that of Schiller's

method [1]

In the matching method the flow field is divided into two sections, the upstream section and downstream section. Schlichting [3], in 1934, solved for the case of laminar flow in the inlet section between parallel plates and found that the boundary layers in the upstream section develop in a way similar to the flow over a flat plate which has a pressure gradient in the direction of flow. The stream function and center line velocity equation are expanded in a power series as in the Blasius' solution[4]. For the downstream section, the velocity is assumed to be the sum of the fully developed parabolic velocity distribution and a deviation velocity obtained by a series expansion in the upstream direction. Having obtained both solutions in the form of a series expansion, they are matched at a point where both solutions are valid.

The velocity profiles obtained by this method are compared with present work in Table 1 and Table 2.

In the finite-difference method the differential equations are approximated by finite-difference equations. Wang and Longwell[5], using finite-difference method, solved for the case of laminar flow in the inlet section between parallel plates without using the usual boundary layer assumptions (ie. neglecting $\frac{\partial^2 u}{\partial x^2}$ and $\frac{\partial p}{\partial y}$). Their analysis was therefore exact in the sense that no term in the momentum equations which are not identically zero were neglected. Their solutions indicated that $\frac{\partial^2 u}{\partial x^2}$ is not negligible relative to $\frac{\partial^2 u}{\partial y^2}$ and the velocity normal to the plates

is not negligible in the vicinity of leading edge.

This report presents a different finite-difference method from that of Wang and Longwell[5]. In this report the continuity equation and the x-momentum equation are used. Moreover, it will be assumed that the pressure gradient is a function of x only and this is introduced into a wall shear force balance equation to find $\frac{dp}{dx}$. The continuity equation, x-momentum equation and the wall shear force balance equation are solved simultaneously.

Since Wang and Longwell[5] eliminated the pressure gradient from the x-momentum and y-momentum equation and introduced a stream function the equation became a fourth-order differential equation. In this report only second-order differential equations were solved so that the computational process was simpler and the solution was approached more economically.

The solution of Wang and Longwell [5] and the present work were compared in Table 1 and Table 2.

III ANALYSIS

The x-axis was taken as center line of the channel and the ordinate y was measured from the center line as shown in Fig. 1.

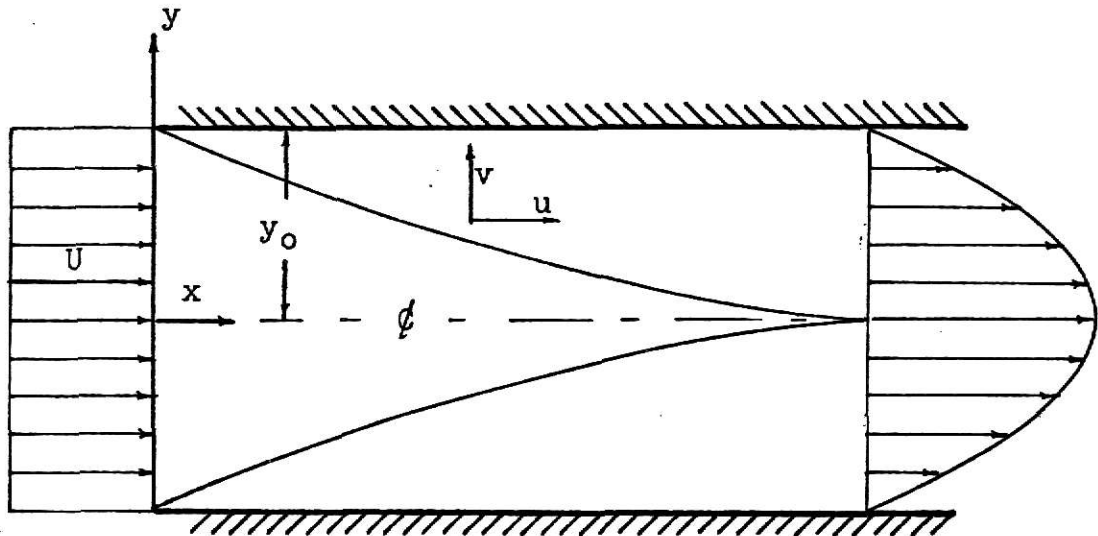


Fig. 1. Geometry of duct-entrance region

The flow was assumed to be steady laminar flow of an incompressible Newtonian fluid between semi-infinite plates. The equation of motion in the x direction was in the form

$$u \frac{\partial u}{\partial x} + v \frac{\partial u}{\partial y} = -\frac{1}{\rho} \frac{\partial p}{\partial x} + \nu \left(\frac{\partial^2 u}{\partial x^2} + \frac{\partial^2 u}{\partial y^2} \right) \quad (1).$$

The equation of continuity was in the form

$$\frac{\partial u}{\partial x} + \frac{\partial v}{\partial y} = 0 \quad (2).$$

Introduced the following dimensionless variable

$$u^+ = \frac{u}{U}, \quad v^+ = \frac{v}{U}, \quad x^+ = \frac{x}{y_0}, \quad y^+ = \frac{y}{y_0}, \quad p^+ = \frac{p}{\rho U^2}$$

and let

$$D = 4y_0, \quad R = \frac{UD}{\nu} = \frac{4y_0 U}{\nu}.$$

Then, the equations of continuity and motion can be written in dimensionless form as

$$\frac{\partial u^+}{\partial x^+} + \frac{\partial v^+}{\partial y^+} = 0 \quad (3)$$

and

$$u^+ \frac{\partial u^+}{\partial x^+} + v^+ \frac{\partial u^+}{\partial y^+} = - \frac{\partial p^+}{\partial x^+} + \frac{4}{R} \left(\frac{\partial^2 u^+}{\partial x^{+2}} + \frac{\partial^2 u^+}{\partial y^{+2}} \right) \quad (4).$$

To give a bounded axial coordinate introduced

$$\eta = 1 - \frac{1}{1+cx^+}$$

where c was a constant and equaled 1.2. The value, $c = 1.2$, was chosen so that the results of this analysis could be directly compared with the results of Wang and Longwell[5].

Then, the equation of continuity can be written

$$\frac{\partial u^+}{\partial \eta} c(1-\eta)^2 + \frac{\partial v^+}{\partial y^+} = 0 \quad (5)$$

and the equation of motion can be written

$$c^2 (1-\eta)^4 \frac{\partial^2 u^+}{\partial \eta^2} + \frac{\partial^2 u^+}{\partial y^{+2}} = \left[2c^2 (1-\eta)^3 + \frac{R}{4} c(1-\eta)^2 u^+ \right] \frac{\partial u^+}{\partial \eta}$$

$$+ \frac{R}{4} v^+ \frac{\partial u^+}{\partial y^+} + \frac{R}{4} c(1-\eta)^2 \frac{\partial p^+}{\partial \eta} \quad (6).$$

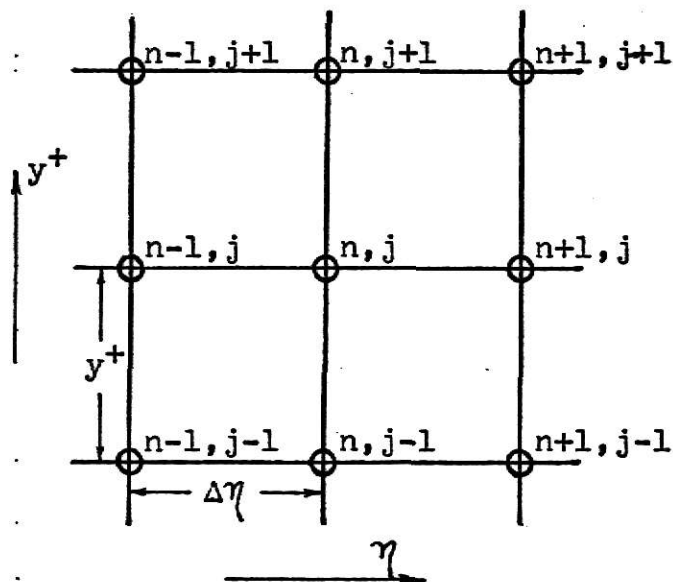
Let

$$c(1-\eta)^2 = \bar{x}$$

Then the equation (6) can be written

$$\begin{aligned} \bar{x}^2 \frac{\partial^2 u^+}{\partial \eta^2} + \frac{\partial^2 u^+}{\partial y^{+2}} &= \left[2c^{\frac{1}{2}} \bar{x}^{\frac{3}{2}} + \frac{R}{4} \bar{x} u^+ \right] \frac{\partial u^+}{\partial \eta} \\ &+ \frac{R}{4} v^+ \frac{\partial u^+}{\partial y^+} + \frac{R}{4} \bar{x} \frac{\partial p^+}{\partial \eta} \end{aligned} \quad (7).$$

Considered Fig. 2, the set of mesh points superimposed on a continuous medium in which three dependent variables, u^+ , v^+ , and p^+ are continuously defined.



where when $j=1, y^+=0$
 $j=j\pi, y^+=1$
 $n=1, \eta=0$
 $n=n\pi, \eta=1$

Fig. 2. Pattern of points

Approximate finite-difference expressions were developed from Taylor's series expansions as follows

$$\frac{\partial^2 u^+}{\partial \eta^2} \Big|_{n,j} = \frac{u_{n-1,j}^+ - 2u_{n,j}^+ + u_{n+1,j}^+}{2} + Q(\Delta \eta^2) \quad (8)$$

$$\frac{\partial u^+}{\partial \eta} \Big|_{n,j} = \frac{u_{n,j+1}^+ - u_{n,j-1}^+}{2 \Delta \eta} + Q(\Delta \eta^2) \quad (9)$$

$$\frac{\partial^2 u^+}{\partial y^{+2}} \Big|_{n,j} = \frac{u_{n,j-1}^+ - 2u_{n,j}^+ + u_{n,j+1}^+}{\Delta y^{+2}} + Q(\Delta y^{+2}) \quad (10)$$

$$\frac{\partial u^+}{\partial y^+} \Big|_{n,j} = \frac{u_{n,j+1}^+ - u_{n,j-1}^+}{2 \Delta y^+} + Q(\Delta y^{+2}) \quad (11)$$

where $Q(\Delta \eta^2)$, $Q(\Delta y^{+2})$ indicated the magnitude of the truncated terms.

Assumed p is a function of x only and from the wall shear force balance we have

$$2p_x y_0 = 2p_{x+dx} y_0 + 2\tau_0 dx$$

where τ_0 was the shear stress at wall.

The above equation can be written

$$\frac{dp}{dx} = - \frac{\tau_0}{y_0} = - \frac{\mu}{y_0} \left(\frac{\partial u}{\partial y} \right)_{n,jpi}$$

or, in dimensionless form,

$$\frac{dp^+}{dx^+} = -\frac{4}{R\bar{x}} \left(\frac{2u^+}{2y^+} \right)_{n,jpi} = -\frac{4}{R\bar{x}} \left(\frac{-3u_{n,jpi}^+ + 4u_{n,jp}^+ - u_{n,jm}^+}{2\Delta y^+} \right) \quad (12)$$

where $jp = jpi - 1$, $jm = jpi - 2$.

Substituting equation (8) through (12) into (7), we had

$$\begin{aligned} \bar{x}^2 \left(\frac{u_{n-1,j}^+ - 2u_{n,j}^+ + u_{n+1,j}^+}{2} \right) + \frac{u_{n,j-1}^+ - 2u_{n,j}^+ + u_{n,j-1}^+}{\Delta y^{+2}} = \\ (2c^{\frac{1}{2}} \bar{x}^{\frac{3}{2}} + \frac{R}{4} \bar{x} u_{n,j}^+) \left(\frac{u_{n,j+1}^+ - u_{n,j-1}^+}{2\Delta\eta} \right) - \frac{4u_{n,jp}^+ - u_{n,jm}^+}{2\Delta y^+} \end{aligned}$$

Solved for $u_{n,j}^+$, we had

$$\begin{aligned} u_{n,j}^+ = \frac{1}{F_{n,j}} \left[\frac{\bar{x}^2 - c^{\frac{1}{2}} \bar{x}^{\frac{3}{2}}}{\Delta\eta^2} u_{n+1,j}^+ + \frac{\bar{x}^2 + c^{\frac{1}{2}} \bar{x}^{\frac{3}{2}}}{\Delta\eta^2} u_{n-1,j}^+ \right. \\ \left. + \frac{8 - Rv_{n,j}^+ \Delta y^+}{8\Delta y^{+2}} u_{n,j+1}^+ + \frac{8 - Rv_{n,j}^+ \Delta y^+}{8\Delta y^{+2}} u_{n,j-1}^+ \right. \\ \left. + \frac{4u_{n,jp}^+ - u_{n,jm}^+}{2\Delta y^+} \right] \quad (13) \end{aligned}$$

where

$$F_{n,j} = \frac{2\bar{x}^2}{\Delta\eta^2} + \frac{2}{\Delta y^{+2}} + \frac{R\bar{x}(u_{n+1,j}^+ - u_{n-1,j}^+)}{8\Delta\eta}$$

Solved $v_{n,j}^+$ from continuity equation

$$\frac{\partial u}{\partial x} + \frac{\partial v}{\partial y} = 0$$

or in dimensionless form,

$$\frac{\partial u^+}{\partial x^+} + \frac{\partial v^+}{\partial y^+} = 0$$

or

$$\frac{\partial u^+}{\partial \eta} c(1-\eta)^2 + \frac{\partial v^+}{\partial y^+} = 0$$

or

$$\frac{\partial u^+}{\partial \eta} \bar{x} + \frac{\partial v^+}{\partial y^+} = 0 \quad (14)$$

or

$$\frac{\partial v^+}{\partial y^+} \Big|_{n,j} = \frac{v_{n,j+1}^+ - v_{n,j}^+}{\Delta y^+} + Q(\Delta y^+) \quad (15)$$

Substituting equation (9) and (15) into (14) we had

$$v_{n,j+1}^+ = v_{n,j}^+ + \frac{\Delta y^+}{2\Delta \eta} \bar{x} (u_{n+1,j}^+ - u_{n-1,j}^+) \quad (16).$$

IV RESULTS

For faster convergence, the program using Simpson's integral started with an initial approximate velocity profile of $v=0$ and u changing linearly from inlet to fully developed flow.

It was found that the solution was unstable at a Reynolds number of 10 when a 10 by 10 grid was used and the solution was stable at a Reynolds number of 300 when 40 by 40 grid was used. The main reason for the instability was truncation error. When a 10 by 10 grid was used the truncated terms $Q(\Delta y^{+2})$ and $Q(\Delta \eta^2)$ were associated with the value of $\Delta y^+ = \Delta \eta = 0.1$. When a 40 by 40 grid was used the truncated terms $Q(\Delta y^{+2})$ and $Q(\Delta \eta^2)$ were associated with the value of $\Delta y^+ = \Delta \eta = 0.025$. Generally the greater the numbers of segments, the better will be the accuracy of numerical approximation.

The velocity profiles and pressure drop found for Reynolds number of 300 were shown in Fig. 3, Fig. 4 and Fig. 5.

The velocity profiles were compared with those of Schlichting [3] and Wang and Longwell [5] at selected locations in Table 1 and Table 2.

It was found that most numerical solutions were between that of Schlichting [3] and Wang and Longwell [5]. The reason for the difference was that Schlichting [3] assumed that pressure was a function of x only and the term $\frac{\partial^2 u}{\partial x^2}$ was neglected but Wang and Longwell [5] solved the differential equation exactly in the sense that no terms have been neglected. In this report, it was assumed

that pressure was a function of x only but the term $\frac{\partial^2 u}{\partial x^2}$ was not neglected.

Figure 4 showed that the velocity component in the y direction was significant near the entrance and the two-dimensional analysis was necessary.

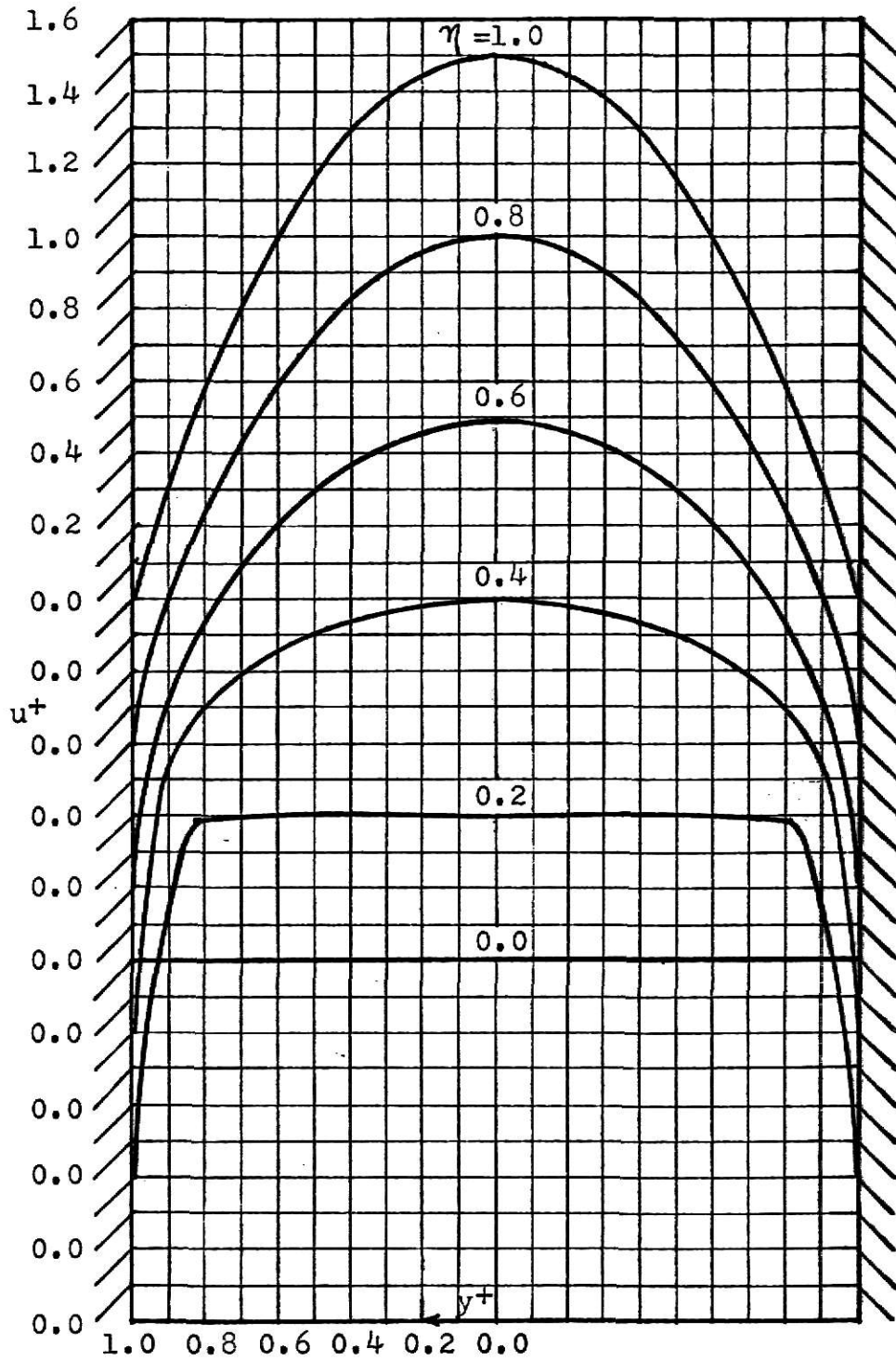


Fig. 3. Velocity profiles

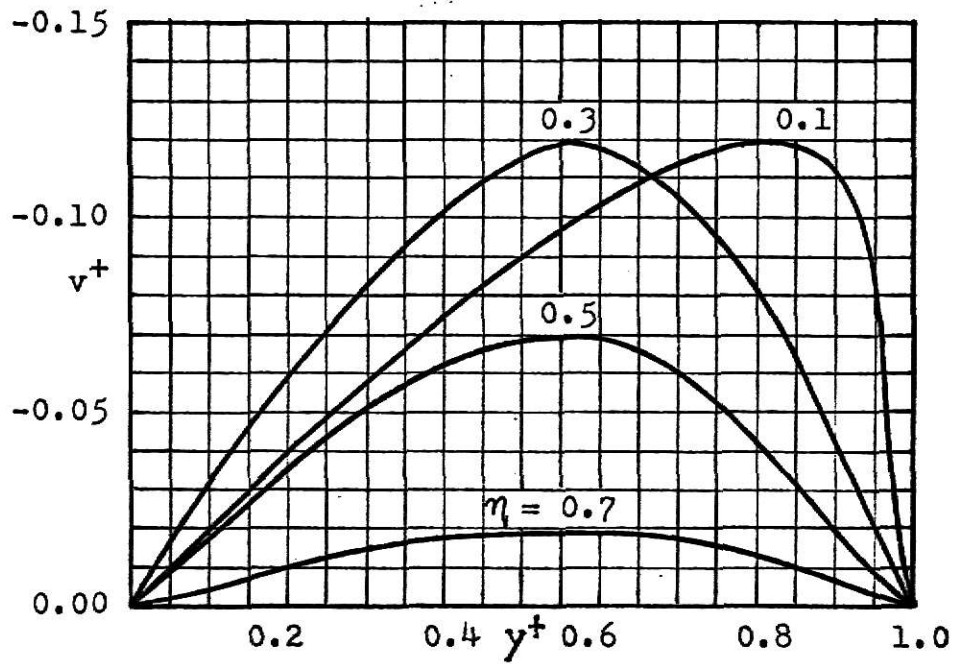


Fig. 4. Velocity profiles

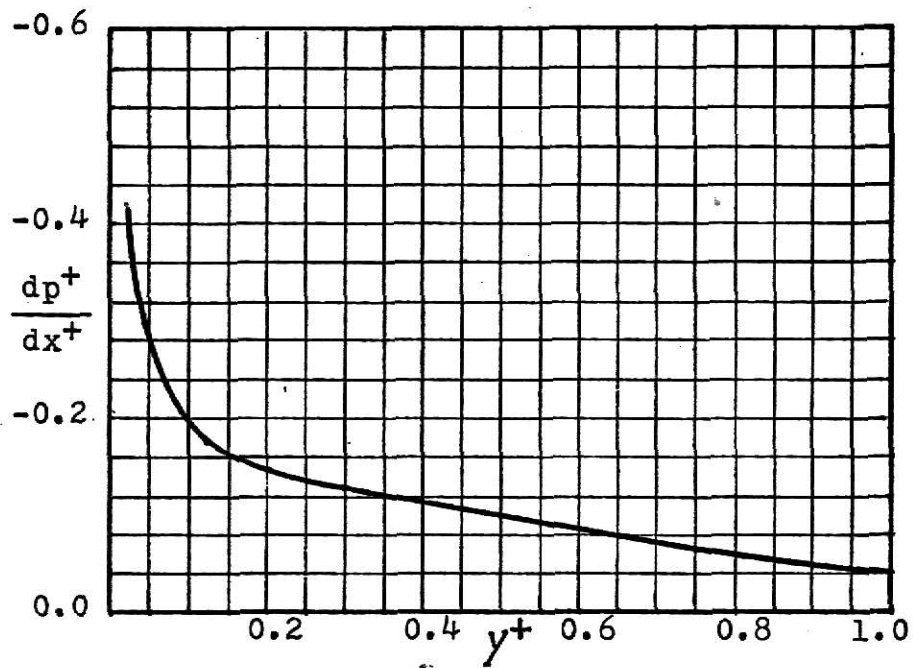


Fig. 5. Pressure distribution

Table 1. Comparison of Results for u^+

$\eta = 0.00 \quad x^+ = 0.0000$			
y^+	Present Work	Schlichting	Wang and Longwell
0.0	1.000	1.000	1.000
0.1	1.000	1.000	1.000
0.2	1.000	1.000	1.000
0.3	1.000	1.000	1.000
0.4	1.000	1.000	1.000
0.5	1.000	1.000	1.000
0.6	1.000	1.000	1.000
0.7	1.000	1.000	1.000
0.8	1.000	1.000	1.000
0.9	1.000	1.000	1.000
1.0	1.000	1.000	1.000
$\eta = 0.20 \quad x^+ = 0.2083$			
y^+	Present Work	Schlichting	Wang and Longwell
0.0	1.081	1.088	1.058
0.1	1.073	1.088	1.059
0.2	1.071	1.088	1.061
0.3	1.068	1.088	1.065
0.4	1.064	1.088	1.071
0.5	1.058	1.088	1.081
0.6	1.051	1.088	1.094
0.7	1.043	1.088	1.105
0.8	1.034	1.046	1.062
0.9	0.906	0.702	0.762
1.0	0.000	0.000	0.000
$\eta = 0.90 \quad x^+ = 7.5000$			
y^+	Present Work	Schlichting	Wang and Longwell
0.0	1.452	1.446	1.451
0.1	1.440	1.436	1.440
0.2	1.400	1.404	1.406
0.3	1.333	1.347	1.347
0.4	1.239	1.261	1.259
0.5	1.118	1.143	1.139
0.6	0.970	0.989	0.965
0.7	0.795	0.797	0.792
0.8	0.593	0.568	0.564
0.9	0.351	0.302	0.300
1.0	0.000	0.000	0.000

Table 2. Comparison of Results for v^+

$\eta = 0.00$ $x^+ = 0.0000$			
y^+	Present Work	Schlichting	Wang and Longwell
0.0	0.0000	0.0000	0.0000
0.1	0.0000	0.0000	0.0000
0.2	0.0000	0.0000	0.0000
0.3	0.0000	0.0000	0.0000
0.4	0.0000	0.0000	0.0000
0.5	0.0000	0.0000	0.0000
0.6	0.0000	0.0000	0.0000
0.7	0.0000	0.0000	0.0000
0.8	0.0000	0.0000	0.0000
0.9	0.0000	0.0000	0.0000
1.0	0.0000	0.0000	0.0000
$\eta = 0.3$ $x^+ = 0.3571$			
y^+	Present Work	Schlichting	Wang and Longwell
0.0	0.0000	0.0000	0.0000
0.1	-0.0320	0.0000	-0.0243
0.2	-0.0600	0.0000	-0.0489
0.3	-0.0843	0.0000	-0.0739
0.4	-0.1036	0.0000	-0.0996
0.5	-0.1158	0.0000	-0.1255
0.6	-0.1185	0.0000	-0.1486
0.7	-0.1090	0.0000	-0.1588
0.8	-0.0844	0.0000	-0.1297
0.9	-0.0418	0.0000	-0.0492
1.0	0.0000	0.0000	0.0000
$\eta = 0.7$ $x^+ = 1.9444$			
y^+	Present Work	Schlichting	Wang and Longwell
0.0	0.0000	0.0000	0.0000
0.1	-0.0055	0.0000	-0.0062
0.2	-0.0108	0.0000	-0.0120
0.3	-0.0154	0.0000	-0.0169
0.4	-0.0188	0.0000	-0.0199
0.5	-0.0206	0.0000	-0.0202
0.6	-0.0206	0.0000	-0.0172
0.7	-0.0183	0.0000	-0.0117
0.8	-0.0135	0.0000	-0.0058
0.9	-0.0060	0.0000	-0.0015
1.0	0.0000	0.0000	0.0000

V REFERENCES

1. L. Schiller, "Die Entwicklung der laminaren Geschwindigkeitsverteilung und ihre Bedeutung für Zähigkeitmessungen," ZAMM, 2, 96-106 (1922).
2. H. L. Langharr, "Steady Flow in the Transition Length of a Straight Tube," Trans. of ASME, J. of Applied Mechanics, 64, A-55 (1942).
3. H. Schlichting, "Laminare Kanuleinaufstromung," ZAMM, 14, 368-373 (1934).
4. H. Schlichting, "Boundary Layer Theory," McGraw-Hill, New York, 6th ed., 125-133 (1966).
5. Y. L. Wang and P. A. Longwell, "Laminar Flow in the Inlet Section of Parallel Plates," AIChE J., Vol. 10, 323-329 (1964).
6. Y. L. Wang and P. A. Longwell, Tabular material has been deposited as document 7846 with the American Documentation Institute, Photoduplication Service, Library of Congress, Washington 25, D. C., and may be obtained for \$2.50 for photoprints or \$1.75 for 35-mm. microfilm.

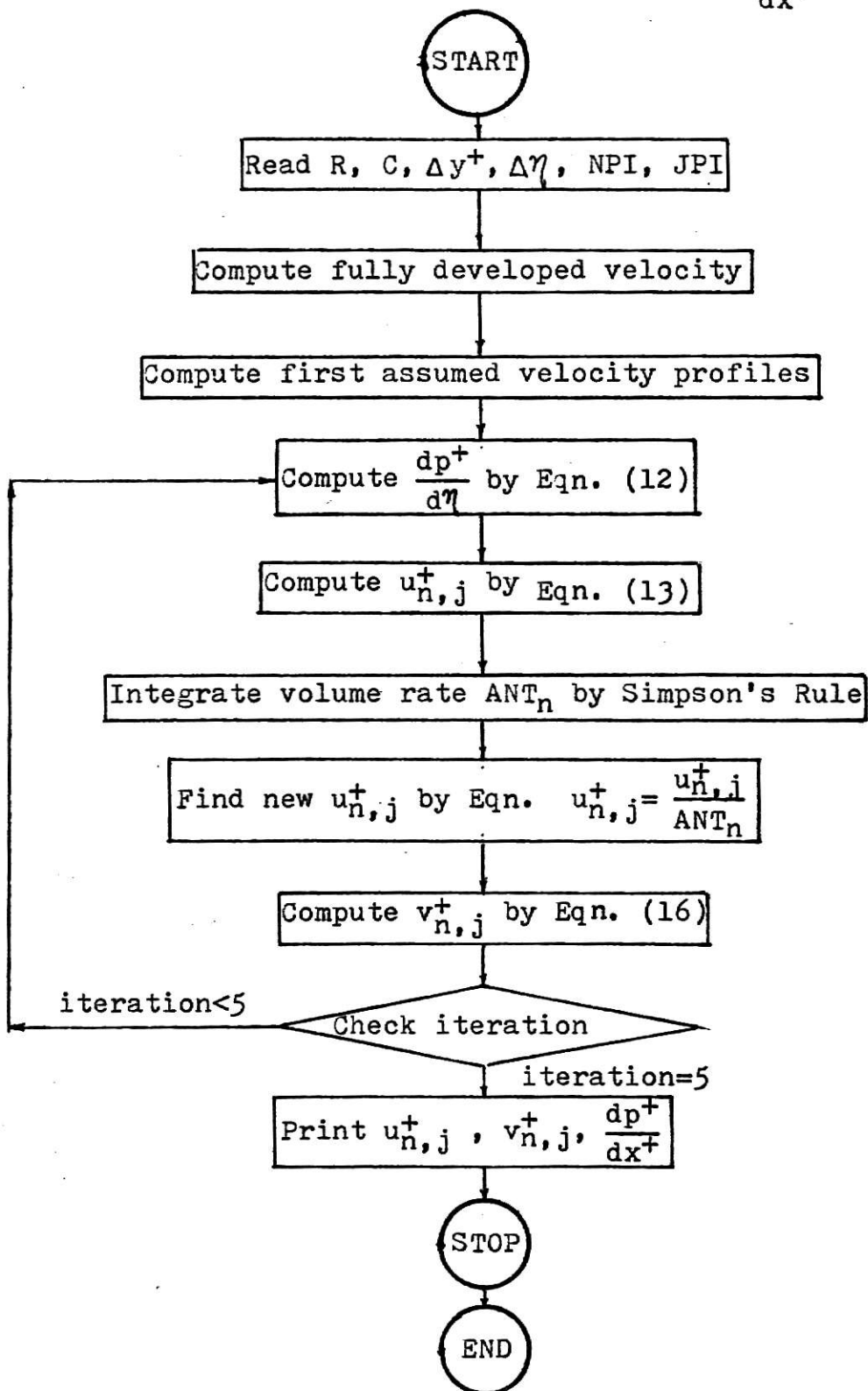
APPENDIX A

Nomenclature

- c = parameter in η transformation, $\eta = 1 - \frac{1}{1+cx^+}$
 D = hydraulic diameter, $D = 4y_0$
 p = pressure
 p^+ = dimensionless pressure, $p^+ = \frac{p}{\rho U^2}$
 R = Reynolds number, $R = \frac{4y_0 U}{\nu}$
 u = x-component of velocity
 u^+ = dimensionless x-component of velocity, $u^+ = \frac{u}{U}$
 U = fluid velocity at inlet
 v = y-component of velocity
 v^+ = dimensionless y-component of velocity, $v^+ = \frac{v}{U}$
 x = cartesian coordinate
 x^+ = dimensionless cartesian coordinate, $x^+ = \frac{x}{y_0}$
 y = cartesian coordinate
 y^+ = dimensionless cartesian coordinate, $y^+ = \frac{y}{y_0}$
 y_0 = duct half width
 d = differential operator
 ∂ = partial differential operator
 Δ = increment in
 η = function of x , $\eta = 1 - \frac{1}{1+cx^+}$
 μ = coefficient of viscosity
 ν = kinematic viscosity
 ρ = fluid density
 τ_0 = wall shear stress

APPENDIX B

Flow Chart for Finding u^+ , v^+ , and $\frac{dp^+}{dx^+}$



APPENDIX C

Program Listing with Selected Output

```

$JOB          GIL,TIME=07,PAGES=20
C
C   THIS PROGRAM SOLVES FOR THE DIMENSIONLESS LAMINAR
C   STEADY HYDRODYNAMIC ENTRANCE REGION VELOCITY PROFILES
C   AND PRESSURE DROP FOR FLOW BETWEEN PARALLEL PLATES
C
1   DIMENSION Y(45), ETA(45), U(45, 45), V(45, 45), DPDETA(45), X(45)
2   2E(45, 45), UI(45), AB(45), ABC(45),DPDX(45) ,ANT(45)
3   10 FORMAT (4F10.5)
4   11 FORMAT (//,35X,'VALUES OF SIMPSON INTEGRAL')
5   20 FORMAT (2I5)
6   12 FORMAT (24X,'*****')
7   21 FORMAT (24X,'*SOME DATA OF U, V, SIMPSON INTEGRAL AND DPDX*')
8   31 FORMAT (24X,'*****')
9   22 FORMAT (/ ,28X,'REYNOLDS NUMBER           R = 300')
10  23 FORMAT (/ ,28X,'NUMBER OF ITERATIONS      I = 5')
11  27 FORMAT (/ ,28X,'TRANSFORMATION CONSTANT C = 1.2')
12  28 FORMAT (/ ,28X,'SQUARE MESH             DY*DETA = 0.025*0.025')
13  24 FORMAT (//,35X,'VELOCITY OF U')
14  25 FORMAT (/ ,15X,6F10.5,/,15X,5F10.5)
15  26 FORMAT (//,35X,'VELOCITY OF V')
16  36 FORMAT (//,35X,'VALUES OF DPDX')
17  READ 10, DETA, DY, C, R
18  READ 20, NPI, JPI
19  DO 30 J = 1, JPI
20  AI=J-1
21  30 Y(J)=AI*DY
22  DO 40 N = 1, NPI
23  BI=N-1
24  40 ETA(N)=BI*DETA
C
C   TO GET INITIAL APPROXIMATE VELOCITY PROFILE ASSUME V=0 AND
C   U CHANGE LINEARLY FROM INLET TO FULLY DEVELOPED FLOW
C
24  DO 50 N = 1, NPI
25  DO 50 J = 1, JPI
26  50 V(N,J) = 0.
27  DO 55 J = 1, JPI
28  55 U(1,J) = 1.
29  DO 60 J = 1, JPI
30  60 U(NPI,J) = 1.5 * (1. - (Y(J))**2)
31  DO 65 N = 2, NPI
32  65 U(N,JPI) = 0.
33  JP = JPI - 1
34  NP = NPI - 1
35  AII = NP

```



```

36      DO 70 J = 1, JP
37      DO 70 N = 1, NP
38      AI = N - 1
39      70 U(N,J) = 1. + (U(NPI,J) - 1. )*AI/AII
      C
      C      COMPUTE VELOCITY PROFILE
      C
40      ITERA=0
41      80 DO 202 J=2,JP
42      DO 202 N=2,NP
43      X(N) = C*(1. - ETA(N))**2
44      JM=JP-1
45      DPDETA(N)=-4.*(4.*U(N,JP)-U(N,JM))/(R*X(N)*2.*DY)
46      FFF = 2.*X(N)**2/DETA**2 + 2./DY**2 + R*X(N)*(U(N+1,J)-U(N-1,J)
      3)/(8.*DETA)
47      AAA = (X(N)**2-C**0.5*X(N)**1.5*DETA)/(FFF *DETA**2)
48      BBB = (X(N)**2+C**0.5*X(N)**1.5*DETA)/(FFF *DETA**2)
49      GGG = (8.-R*V(N,J)*DY)/(FFF *8.*DY**2)
50      DDD = (8.+R*V(N,J)*DY)/(FFF *8.*DY**2)
51      EEE = (4.*U(N,JP)-U(N,JM))/(2.*DY*FFF)
52      200 U(N,J) = AAA*U(N+1,J) + BBB*U(N-1,J) + GGG*U(N,J+1)
      4+DDD*U(N,J-1)+EEE
53      202 CONTINUE
54      DO 203 N=1,NPI
55      203 U(N,1)=-U(N,3)/3.+4.*U(N,2)/3.
56      DO 300 N = 1, NPI
57      DO 250 J=1,JPI
58      250 UI(J)=U(N,J)
      C
      C      SIMPSON'S RULE INTEGRATION FOR THE BULK VELOCITY
      C
59      CALL SIMPI (UI,JPI,AAT)
60      300 ANT(N)=AAT
      C
      C      MODIFY THE VELOCITY PROFILE TO GIVE CONSISTENT RESULTS
      C
61      DO 400 N = 2, NP
62      DO 400 J=1,JP
63      400 U(N,J) = U(N,J)/ANT(N)
64      DO 500 N = 2, NP
65      JPA=JP-1
66      DO 500 J=1,JPA
67      500 V(N,J+1)=V(N,J)-DY*C*(1.-ETA(N))**2*(U(N+1,J)-U(N-1,J))/(2.*DETA)
68      DPDX(1)=0.
69      DO 502 N=2,NPI
70      502 DPDX(N)=-4.*(4.*U(N,JP)-U(N,JM))/(R*2.*DY)

```

```

71     ITERA=ITERA+1
72     IF (ITERA.LT.5) GO TO 80
73     WRITE (3,12)
74     WRITE (3,21)
75     WRITE (3,31)
76     WRITE (3,22)
77     WRITE (3,23)
78     WRITE (3,27)
79     WRITE (3,28)
80     WRITE(3,24)
81     DO 705 J=1,JPI,4
82 705 WRITE(3,25)(U(N,J),N=1,NPI,4)
83     WRITE(3,11)
84     WRITE(3,25)(ANT(N),N=1,NPI,4)
85     WRITE(3,26)
86     DO 805 J=1,JPI,4
87 805 WRITE(3,25)(V(N,J),N=1,NPI,4)
88     WRITE(3,36)
89     WRITE(3,25)(DPDX(N),N=1,NPI,4)
90     STOP
91     END

```

```

92     SUBROUTINE SIMPI(F,NPL,RESULT)
93     DIMENSION F(25)
94     NH=(NPL-1)/2-1
95     H=NPL-1
96     H=1.0/H
97     SUM=0.0
98     DO 1 J=1,NH
99 1 SUM=SUM+4.*F(2*J)+2.*F(2*J+1)
100     RESULT=(SUM+F(1)+4.*F(NPL-1)+F(NPL))*H/3.
101     RETURN
102     END

```

 SOME DATA OF U, V, SIMPSON INTEGRAL AND DPDX

REYNOLDS NUMBER R = 300
 NUMBER OF ITERATIONS I = 5
 TRANSFORMATION CONSTANT C = 1.2
 SQUARE MESH DY*DETA = 0.025*0.025

VELOCITY OF U

1.00000	1.05725	1.08105	1.12814	1.18863	1.24796
1.30281	1.35442	1.40392	1.45218	1.50000	
1.00000	1.04977	1.07328	1.11284	1.17039	1.23330
1.29189	1.34490	1.39385	1.44019	1.48500	
1.00000	1.04932	1.07055	1.10581	1.15670	1.21381
1.26764	1.31567	1.35941	1.40051	1.44000	
1.00000	1.04921	1.06779	1.09733	1.13909	1.18486
1.22767	1.26583	1.30064	1.33343	1.36500	
1.00000	1.04884	1.06371	1.08491	1.11382	1.14390
1.17121	1.19558	1.21803	1.23934	1.26000	
1.00000	1.04820	1.05816	1.06802	1.07978	1.08989
1.09781	1.10485	1.11163	1.11832	1.12500	
1.00000	1.04729	1.05117	1.04645	1.03627	1.02201
1.00696	0.99340	0.98136	0.97035	0.96000	
1.00000	1.04610	1.04290	1.02023	0.98275	0.93951
0.89810	0.86091	0.82708	0.79539	0.76500	
1.00000	1.04469	1.03373	0.98977	0.91881	0.84169
0.77069	0.70706	0.64862	0.59340	0.54000	
1.00000	0.97158	0.90629	0.83015	0.73831	0.64683
0.56459	0.48979	0.41940	0.35150	0.28500	
1.00000	0.00000	0.00000	0.00000	0.00000	0.00000
0.00000	0.00000	0.00000	0.00000	0.00000	

VALUES OF SIMPSON INTEGRAL

1.00000	0.99343	0.99793	0.99761	0.99655	0.99685
0.99788	0.99882	0.99949	0.99989	1.00000	

VELOCITY OF V

0.00000	0.00000	0.00000	0.00000	0.00000	0.00000
0.00000	0.00000	0.00000	0.00000	0.00000	
0.00000	-0.02036	-0.02513	-0.03205	-0.02691	-0.01768
-0.01042	-0.00549	-0.00233	-0.00057	0.00000	
0.00000	-0.04024	-0.04716	-0.06003	-0.05299	-0.03575
-0.02085	-0.01080	-0.00453	-0.00109	0.00000	
0.00000	-0.05876	-0.06663	-0.08438	-0.07551	-0.05152
-0.02993	-0.01538	-0.00641	-0.00154	0.00000	
0.00000	-0.07577	-0.08245	-0.10368	-0.09280	-0.06330
-0.03668	-0.01879	-0.00783	-0.00188	0.00000	
0.00000	-0.09074	-0.09317	-0.11584	-0.10304	-0.06982
-0.04035	-0.02067	-0.00861	-0.00207	0.00000	
0.00000	-0.10312	-0.09720	-0.11849	-0.10425	-0.06984
-0.04024	-0.02064	-0.00862	-0.00207	0.00000	
0.00000	-0.11241	-0.09298	-0.10898	-0.09427	-0.06222
-0.03572	-0.01838	-0.00770	-0.00186	0.00000	
0.00000	-0.11820	-0.07914	-0.08441	-0.07071	-0.04580
-0.02622	-0.01356	-0.00571	-0.00138	0.00000	
0.00000	-0.11587	-0.05246	-0.04181	-0.03163	-0.01996
-0.01147	-0.00602	-0.00257	-0.00063	0.00000	
0.00000	0.00000	0.00000	0.00000	0.00000	0.00000
0.00000	0.00000	0.00000	0.00000	0.00000	

VALUES OF DPDX

0.00000	-0.18768	-0.15013	-0.13047	-0.11359	-0.09851
-0.08536	-0.07344	-0.06209	-0.05099	-0.04000	

HYDRODYNAMIC ENTRANCE REGION FLOW OF A PARALLEL PLATE CHANNEL

by

WEI-CHUNG CHEN

B. S., National Taiwan University, 1968

AN ABSTRACT OF A MASTER'S REPORT

subitted in partial fulfillment of the

requirments for the degree

MASTER OF SCIENCE

Department of Civil Engineering

KANSAS STATE UNIVERSITY
Manhattan, Kansas

1970

ABSTRACT

The developing steady laminar flow of an incompressible fluid in a parallel plate channel is considered.

The velocity profiles and pressure distribution in the hydrodynamic entrance region are determined by a finite-difference method.

The numerical solutions are compared with the solutions of other authors.